Journal of the Serbian Chemical Society
JSCS-info@shd.org.rs • www.shd.org.rs/JSCS

ACCEPTED MANUSCRIPT

Journal of the Serbian Chemical Society
JSCS-info@shd.org.rs • www.shd.org.rs/JSCS
J. Serb. Chem. Soc. **00(0)** 1-14 (2026)
JSCS–13950
Original scientific paper
Published DD MM, 2026

Projection of the liquidus surface of the Ag_2S–In_2S_3–FeS quasi-ternary system

IKHTIYAR B. BAKHTIYARLY*, SHAHRI S. ABDULLAYEVA, RUKSANA C. QURBANOVA, VILAYET S. MAMMADOV, ELNARA N. ISMAYILOVA

Institute of Catalysis and Inorganic Chemistry named after academician M. Naghiyev of the Ministry of Science and Education of the Republic of Azerbaijan, Baku, Azerbaijan.

(Received 4 May; revised 4 June; accepted 13 August 2026)

Abstract: The complex methods of physicochemical analysis, including differential thermal analysis (DTA), X-ray diffraction analysis (XRD), microstructure analysis (MSA), as well as measurements of microhardness and density, have been applied to investigate the Ag_2S–In_2S_3–FeS quasi-ternary system along the polythermal section for the first time. The nature of the chemical interactions within the system has been identified, and the phase diagram of the polythermal section, as well as the projection of the liquidus surface of the quasi-ternary system, has been constructed. In the investigated system, the coordinates of nonvariant points, monovariant curves, the boundaries of primary crystallization fields, and isotherms have been determined. It has been established that the system comprises six primary crystallization fields, which are bounded by seven monovariant curves. Among the ten nonvariant equilibria identified in the system, seven are attributed to three-phase binary eutectic, one to a three-phase binary peritectic, one to a four-phase ternary peritectic, and one to a four-phase ternary eutectic reaction.

Keywords: quasi-binary system; eutectic; monovariant; nonvariant; congruent; optical detector.

INTRODUCTION

Silver and indium chalcogenides, in particular their ternary compounds with magnetic ions of these elements and solid solutions based on them, are among the most important functional materials for modern electronics and other high technologies. Many of these materials have gained significant importance in recent decades as photoelectric, optical, thermoelectric, magnetic, and catalytic properties and are considered promising for use in the electronics industry.[1-5]

$AgInS_2$, $AgIn_5S_8$, and $FeIn_2S_4$ compounds are unconventional semiconductor materials due to their optical and electrical properties and have found important

* Corresponding author. E-mail: ibbakhtiyarli@mail.ru
https://doi.org/10.2298/JSC260504047B

applications in modern technologies fields. Their advantages in optoelectronics and nanomaterials are closely related, to their high photoelectric properties. These, which are solar converters can be used in laser and optical detector systems in the infrared spectrum range and compared to traditional converters, provide higher energy conversion efficiency with lower material consumption. The stable operating characteristics of these materials at high temperatures and electric fields make them suitable for use in transistors, diodes, sensors, and other semiconductor components.[6-11] The most interesting application of $AgInS_2$ and $FeIn_2S_4$ compounds is their use in the development of biosensors for biotechnology. These biosensors are used to measure changes at the cellular level or to detect microorganisms for biological analysis and disease diagnosis based on the principle of light absorption and increased photoluminescence intensity.[12-14]

However, since the composition of these compounds is in most cases determined empirically through numerous experiments, this creates certain difficulties in their synthesis, thermal processing, selection of processing intervals, and determination of optimal compositions.

This article of scientific and practical importance is dedicated to determining the nature of the chemical interactions in the $Ag_2S–In_2S_3–FeS$ quasi-ternary system, construct the projection of the liquid surface and study the physicochemical properties of the new phases obtained individually from the system. The projection of the liquidus surface of the $Ag_2S–In_2S_3–FeS$ quasi-ternary system has not been studied in the literature data. However, T-x phase diagrams of the $Ag_2S–In_2S_3$, $In_2S_3–FeS$, and $Ag_2S–FeS$ quasi-binary systems have been constructed in the reference constitute it.

The phase diagram of the $Ag_2S–In_2S_3$ system,[15] is quasi-binary. Two new phases are formed in the system: $AgInS_2$ and $AgIn_5S_8$. $AgInS_2$ melts incongruently formed as a result of a peritectic reaction at 1130 K. The $AgIn_5S_8$ compound melts congruently at 1360 K and forms a continuous solid solution with In_2S_3. According to literature,[16] the compound $AgIn_{11}S_{17}$ is not shown on the diagram, because it is dissolved in the homogeneity field of the solid solution. The coordinates of the eutectic points in the system are 13 mol% In_2S_3 at 943 K and 94.5 mol% In_2S_3 at 1336 K. At room temperature, the solubility in Ag_2S is 2 mol% In_2S_3. However, the solubility based on In_2S_3 was no practically observed.

$AgInS_2$ crystallizes in a tetragonal structure of the chalcopyrite type with space group $I\bar{4}2d$ and lattice parameters a=5.88; c=11.20 Å.[17] $AgIn_5S_8$ crystallizes in the cubic structure (sp. gr. $F\bar{d}3m$) a= 8.22 Å.[18]

T-x diagram of the $FeS–In_2S_3$ system is quasi-binary.[19] $FeIn_2S_4$ congruently melting forms at 1398 K at 1:1 ratio of the initial components. A eutectic equilibrium is established at 73 mol.% FeS and 1373 K. The alloy forms a continuous solid solution region with a minimum extremum (14 mol.% FeS) in the composition range 0–55 mol.% FeS. $FeIn_2S_4$ crystallizes in a cubic spinel structure,

a=10.53. Å.[19] The phase diagram of the Ag_2S–FeS system is quasi-binary.[20] The system is of the simple eutectic type. The eutectic composition is 87 mol.% Ag_2S, and its temperature is 893 K. Solution based on initial components has not been observed.

EXPERIMENTAL

In our experiments, α–Ag_2S, β–In_2S_3, and β–FeS were used as initial components. α–Ag_2S crystallizes in the monoclinic system with lattice parameters space group $P2_1/c$, *a*=4.2264, *b*=6.9282, *c*=9.5317 Å, and β=125.554°, *Z*=4.[21]

β–In_2S_3 crystallizes in the tetragonal syngony, with space group $I4_1/amd$ and lattice parameters *a*=7.623, *c*=32.36 Å, *Z*=16.[22]

β–FeS crystallizes in the hexagonal syngony with a troilite-type structure. The lattice parameters are *a*=5.962, *c*=11.75 Å, and the space group is $P\bar{6}2c$ with *Z*=12.[23]

The initial components were synthesized from the elements (Fe -reduction, In-000, Ag-99.9 wt.% and S-99.9999 wt.%, special purity) in an evacuated quartz ampoule by the visually controlled combined direct method in a two-zone furnace.

Samples, composed of the appropriate components in stoichiometric amounts were also synthesized by the direct method. It should be noted that FeS and FeS-rich alloys were synthesized in a graphitized thick-walled ampoule (or in a quartz ampoule containing a glassy-graphite crucible). During the synthesis process, the furnace is heated to 800 K. Then, the ampule is inserted into the furnace and temperature is gradually increased until it is 30–40 degrees above the melting point of the obtained substance. Sample is synthesized within 3 hours at this temperature and gradually cooled. To homogenize the sample, it is heat-treated for 200 hours at the temperature 50 degrees below the liquidus curve.

After each experiment, the homogeneity of the synthesized samples is confirmed by method of microstructural (MSA) and X-ray diffraction analysis (XRD). Also, alloys of the Ag_2S–In_2S_3–FeS quasi-ternary system were investigated by using physicochemical analysis methods: differential thermal (DTA), XRD and MSA analysis, as well as by methods for measuring microhardness and density.[24-26]

DTA was performed under dynamic conditions in an inert environment (He) using a NETZSCH STA 449 F3 Jupiter synchronous thermal analysis system (using a Pt-Pt/Rh thermocouple, the heating rate was 15 degrees/min). The standard Proteus (R) Software was used for device control.[27,28] The accuracy of the instrument is ±2 degrees at 1400 K.

XRD was conducted at room temperature on a “D2 Phaser” with CuKα radiation, Ni filter (Bruker, Germany). The scanning speed was 2 degrees/min. The DIFFAC.SUITE proprietary software package was used for instrument control and data analysis.

MSA analysis was performed on the polished surface using the METAM-PB, manufactured by OAO “LOMO”, and the MC-500 microscope, which belongs to the Austrian company “Mikros”.[29]

In studying the microstructure of the alloys, an etchant comprising NH_4NO_3 (3–8 wt.%), $K_2Cr_2O_7$ (0.02–0.5 wt.%), and concentrated H_2SO_4 was used (etching time 20 s). Microhardness measurements were carried out using a PMT-3 microhardness tester. The density at 300 K was determined by the pycnometric method, with toluene used as the filling liquid.

RESULTS AND DISCUSSION

The chemical interactions in the quasi–ternary Ag_2S–In_2S_3–FeS system have been investigated using quasi-binary systems, including $AgIn_5S_8$–$FeIn_2S_4$ ($AgIn_5S_8$

– $(3In_2S_3)_{0.895}(5Ag_2S)_{0.105}$; $FeIn_2S_4$ – $(3In_2S_3)_{0.714}(7.5FeS)_{0.286}$); $AgIn_5S_8$–7.5FeS; $5Ag_2S$–M (M – $(3In_2S_3)_{0.69}(7.5FeS)_{0.227}(5Ag_2S)_{0.083}$); M–$FeIn_2S_4$, A–$3In_2S_3$ (A – $(5Ag_2S)_{0.50}(7.5FeS)_{0.50}$); S–7.5FeS (S – $AgInS_2$ – $(3In_2S_3)_{0.62}(5Ag_2S)_{0.38}$); e_7–e_5 (e_7 – $(5Ag_2S)_{0.915}(7.5FeS)_{0.085}$; e_5 –$(3In_2S_3)_{0.465}(7.5FeS)_{0.475}(5Ag_2S)_{0.060}$) along polythermal internal section.

$AgIn_5S_8$–$FeIn_2S_4$ section

The phase diagram of the $AgIn_5S_8$–$FeIn_2S_4$ system was first investigated by Olekseyuk et al.[30] According to their study, the system is quasi-binary and forms a continuous solid solution over the entire composition range (Fig. 1).

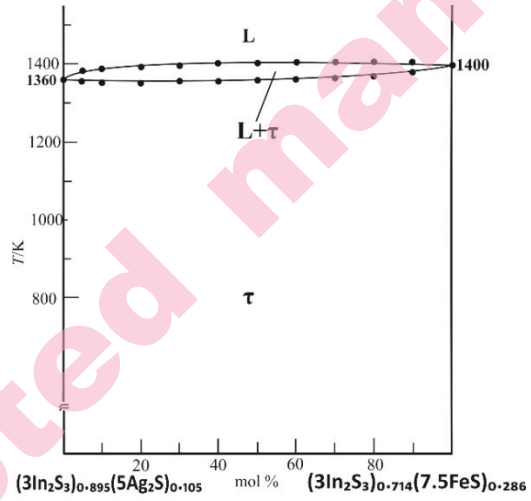

Fig. 1. The phase diagram of the $AgIn_5S_8$–$FeIn_2S_4$ system.

This solid solution crystallizes in the spinel structure type ($MgAl_2O_4$, space group $Fd\bar{3}m$) within the cubic symmetry. The dependence of the lattice parameters on the composition shows that depending on the concentration of $FeIn_2S_4$, the lattice constant of the solid solution varies monotonically within the range of 10.831 to 10.629 Å.[31] A single crystal of the solid solution with the composition $(AgIn_5S_8)_{0.50}(FeIn_2S_4)_{0.50}$ was grown using the Bridgman method, and no diffraction lines deviating from the spinel-type cubic symmetry were observed in the diffractogram. This condition confirms the presence of a continuous solid solution within the system.

$AgIn_5S_8$-7.5FeS section

The phase diagram of the $AgIn_5S_8$–7.5FeS section is quasi-binary (Fig. 2). The liquidus curve consists of two branches corresponding to the primary crystallization of τ and γ (FeS) phases. A solid solution region based on $AgIn_5S_8$

(τ) is observed, with a maximum extremum (M) over a wide composition range (0–29 mol.% 7.5FeS).

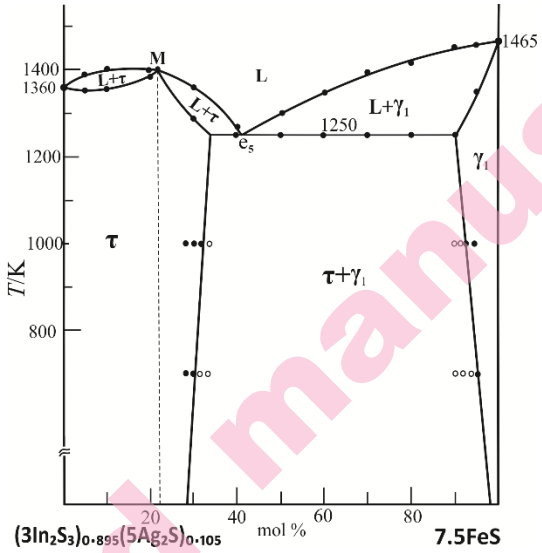

Fig. 2. The phase diagram of the $AgIn_5S_8$–7.5FeS system.

The coordinates of the extremum point are 22.7 mol.% 7.5FeS (or M – 69.0 mol.% $3In_2S_3$, 8.3 mol.% $5Ag_2S$, 22.7 mol.% 7.5FeS) and a temperature of 1400 K. It is observed that at the extremum point, the liquidus and solidus curves intersect, and at this point, the compositions of the solid and liquid phases are identical, satisfying the phase rule. According to this rule, a binary system consisting of two phases with identical compositions behaves as a pseudo- single-component system. Therefore, these are conditionally considered as a nonvariant system.[32] The coordinates of the eutectic equilibrium between the solid solution and FeS are 46.575 mol.% 7.5FeS (47.425 mol.% $3In_2S_3$, 6 mol.% $5Ag_2S$), and temperature of 1230 K. There is a solubility of 3 mol.% $AgIn_5S_8$ (γ_1) in FeS. As a result of these processes, a mixture of two phases (τ + γ_1) is formed in the subsolidus.

The primary crystallization field of the solid solution with an extremum M occupies a large area in the projection of the liquidus surface. The formation of this extensive region appears to result from the mixing with each other of the primary crystallization fields of solid solutions based on $AgIn_5S_8$, β–In_2S_3, and $FeIn_2S_4$. This phenomenon is likely related with the isostructural crystallization of these compounds in the cubic spinel lattice and their similar lattice parameters (a=10.82 Å;[18] a=10.78 Å;[33] a=10.60 Å[19]). In the experimental section, it is noted that β–In_2S_3 crystallizes in a tetragonal symmetry, as investigated in the study of its crystal structure. However, in the literature,[22] this modification is reported to

crystallize in the cubic system with a cation-deficient γ–Al_2O_3 spinel structure type, and by different authors,[34-36] have reported lattice parameters in the range of 10.724÷10.78 Å. It appears that, although this compound may be indexed in different symmetries, it is the same material. A simple planar reconstruction relationship exists between these structures, allowing an easy transition via slight collective atomic displacements.[37,38]

To further clarify the nature of the chemical interactions, the conditionally nonvariant maximum extremum point M–$(3In_2S_3)_{0.69}(7.5FeS)_{0.227}(5Ag_2S)_{0.083}$ was investigated along with two additional sections: $5Ag_2S$–M and $FeIn_2S_4$–M.

$5Ag_2S$-M section

The phase diagram of the $5Ag_2S$-M section (Fig. 3) shows that the projection of the liquidus surface passes through three primary crystallization fields. Accordingly, the liquidus curve consists of three branches (α, S, τ). Two of these branches (α and S) intersect at the eutectic point e_6. In the subsolidus region, α + S assemblage crystallizes. The composition of the e_6 is $(5Ag_2S)_{0.8258}(3In_2S_3)_{0.1311}(7.5FeS)_{0.0431}$, and its temperature is 910 K.

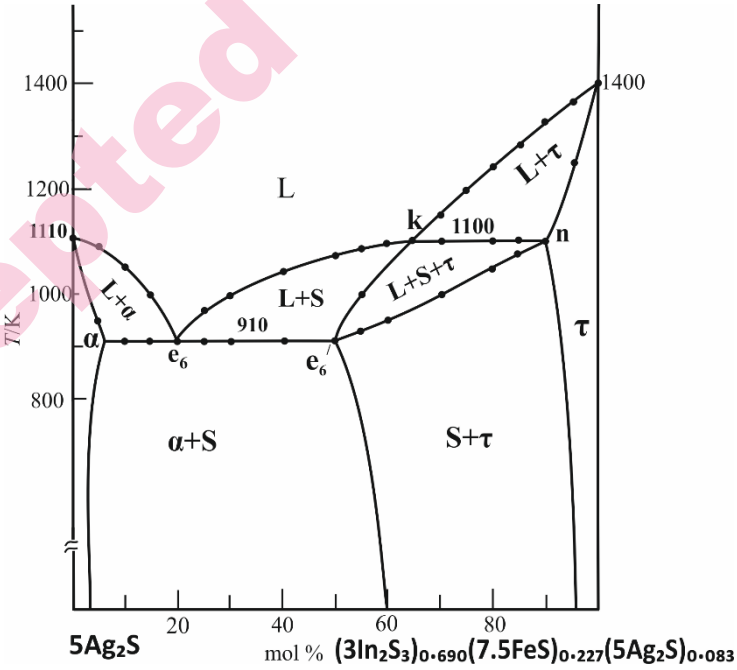

Fig. 3. The phase diagram of the $5Ag_2S$–M system

In the section of the liquidus surface projection, the peritectoid-type (pP) monovariant curve is intersected at point k, where the binary crystallization reaction L ↔ S + τ occurs. This process completed along the $e_6'n$ subcurve,

resulting in the precipitation of a two-phase mixture (S + τ) in the subsolidus region. The limited solubility based on initial components was observed in the phase diagram. Considering that, in the subsolidus region, a three-phase field (L + S + τ) exists in the composition range of 50÷100 mol.% M, this section can be regarded as partially quasi-binary.

M–$FeIn_2S_4$ section

The phase diagram of the M–$FeIn_2S_4$ section is also quasi-binary (Fig. 4). A continuous solid solution exists between two components.

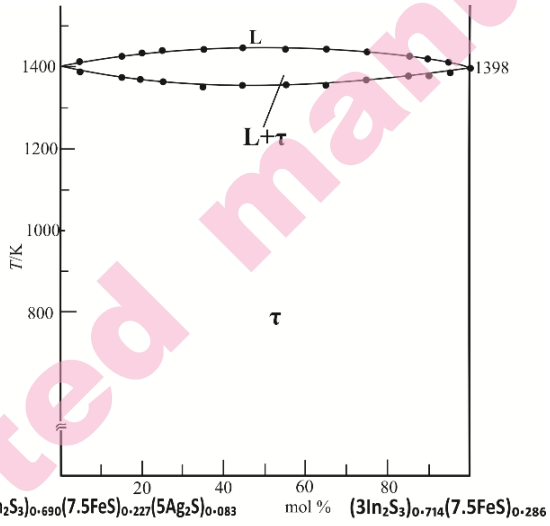

Fig. 4. The phase diagram of the M-$FeIn_2S_4$ system

Based on the investigated quasi-binary sections, the Ag_2S-In_2S_3-FeS quasi-ternary system was singularly triangulated and divided into three ternary subsystems: Ag_2S–$AgIn_5S_8$–FeS, $AgIn_5S_8$–$FeIn_2S_4$–FeS and $AgIn_5S_8$–In_2S_3–$FeIn_2S_4$. Since the common side $AgIn_5S_8$- $FeIn_2S_4$ of the $AgIn_5S_8$–In_2S_3–$FeIn_2S_4$ and $AgIn_5S_8$–$FeIn_2S_4$–FeS systems forms a continuous solid solution over its entire composition range, crystallization in this region does not terminate at the ternary nonvariant equilibrium point (E) shown in the projection of the liquidus surface. Instead, it proceeds to completion along the corresponding e_1p and e_4e_5 monovariant curves. In the subordinate triangle Ag_2S–$AgIn_5S_8$–FeS, the process is comparatively more complex; this will be discussed in detail in the projection of the liquidus surface. To determine the coordinates of nonvariant points, monovariant curves, isotherms, and the boundaries of primary crystallization fields in the projection of the liquidus surface of Ag_2S–In_2S_3–FeS quasi-ternary system, a series of non-quasibinary sections were investigated. Some of these will be considered in detail.

A–3In$_2$S$_3$ section

The A–3In$_2$S$_3$ is a non-quasibinary section of the quasi-ternary system (Fig. 5). The composition at point A (5Ag$_2$S)$_{0.50}$(7.5FeS)$_{0.50}$) corresponds to a mechanical mixture in the 5Ag$_2$S–7.5FeS quasi-binary system, with a melting temperature of 1330 K.

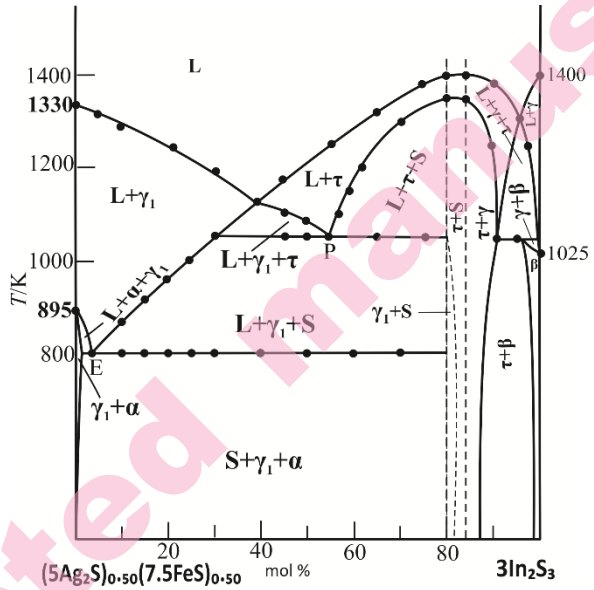

Fig. 5. The phase diagram of the A–3In$_2$S$_3$ system

Consequently, the phase diagram of the A-3In$_2$S$_3$ section is divided into three regions, and the liquidus of the system consists of three branches corresponding to the primary crystallization fields (γ_1, τ, γ). These branches converge at the points where the A–In$_2$S$_3$ section intersects the monovariant curves. Within the region of the section corresponding to the Ag$_2$S–AgIn$_5$S$_8$–FeS subordinate ternary system, the nature of chemical interactions is relatively complex. In this region, the coordinates of the only ternary nonvariant peritectic equilibrium [P: L + τ(AgIn$_5$S$_8$) ↔ S(AgInS$_2$) + γ_1(FeS)] and the ternary eutectic equilibrium [E: L ↔ γ_1(FeS) + α(Ag$_2$S) + S(AgInS$_2$)] are established as follows: P: 39.0 mol% In$_2$S$_3$, 24.50 mol.% 7.5FeS, 36.50 mol.% 5Ag$_2$S, at T = 1050 K; E: 5.00 mol.% 3In$_2$S$_3$, 7.00 mol.% 7.5FeS, 88.00 mol.% 5Ag$_2$S, at T = 800 K.

In the concentration range of 0÷80 mol.% In$_2$S$_3$ crystallization is completed at the E invariant eutectic equilibrium. In the portion of the section passing through the AgIn$_5$S$_8$–FeIn$_2$S$_4$–FeS and AgIn$_5$S$_8$–In$_2$S$_3$–FeIn$_2$S$_4$ subordinate triangles, as noted above, crystallization does not terminate at a ternary invariant equilibrium; rather, it proceeds to completion along the monovariant curves e$_1$p and e$_4$e$_5$, respectively. The mixed of S + γ_1 + α phases precipitate in the subsolidus.

S-7.5FeS section

The S($AgInS_2$)–7.5FeS section is non-quasibinary (Fig. 6). It passes through the field of the Ag_2S-$AgIn_5S_8$-FeS ternary system and intersects two primary crystallization regions (τ and γ_1). Therefore, the liquidus curve consists of two branches corresponding to these phases.

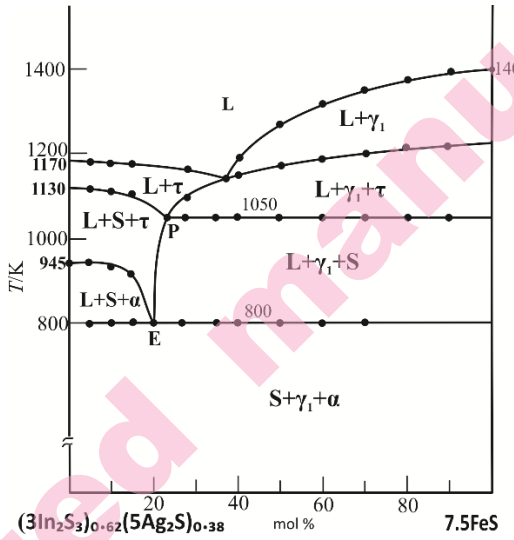

Fig. 6. The phase diagram of the S-7.5FeS

These branches intersect at the point where the monovariant curve of the section crosses (at 37 mol.% FeS concentration and 1140 K), and at that point τ + γ_1 initial crystallization begins. In the subliquidus region, crystallization proceeds through a four-phase ternary peritectic and concludes in a four-phase ternary eutectic equilibrium (at 800 K). In the subsolidus region, the S + γ_1 + α phase mixture precipitates. In the phase diagram of the section, there are binary crystallization regions depending on the composition, such as S + τ, γ_1 + τ, S + α, and γ_1 + S.

e_7-e_5 section

The phase diagram of the e_7–e_5 section is non-quasibinary (Fig. 7). The selected initial components correspond to eutectic compositions in the $5Ag_2S$–7.5FeS and $AgIn_5S_8$–FeS quasibinary sections. This section passes through the region of the Ag_2S–$AgIn_5S_8$–FeS subordinate ternary system and intersects only the γ_1 (FeS) primary crystallization field. Therefore, its liquidus consists of a single branch.

In the 70–100 mol.% e_5 concentration range, a four-phase ternary peritectic equilibrium is observed at 1050 K. In the subliquidus region, the phase diagram exhibits the binary crystallization fields α + γ_1, γ_1 + S, and γ_1 + τ. Crystallization is

completed via a four-phase ternary eutectic equilibrium across the entire concentration range. In the subsolidus region, an S($AgInS_2$) + γ_1 (FeS) + α(Ag_2S) phase assemblage is formed.

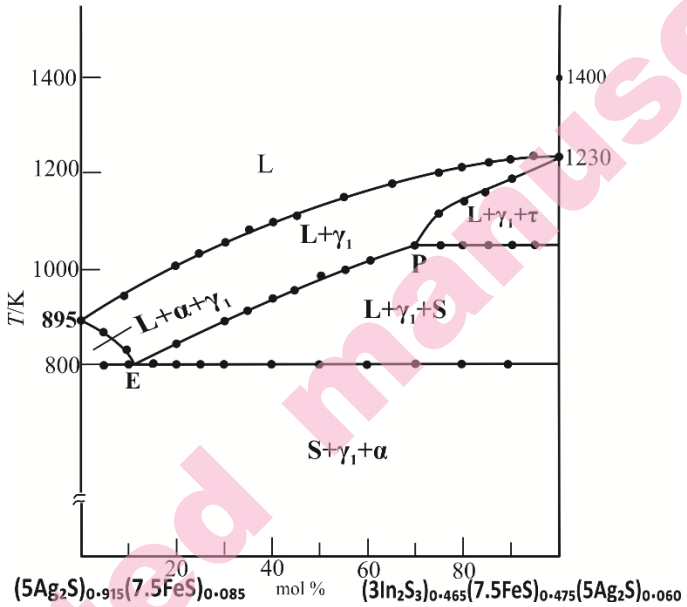

Fig. 7. The phase diagram of the e_7–e_5 system

The consistency of chemical interactions at the intersection points of the investigated quasi-binary and non-quasibinary polythermal sections confirms the reliability of the results. Based on the study of these sections, along with additional samples not intersecting them, the projection of the liquidus surface of the Ag_2S–In_2S_3–FeS ternary system was constructed (Fig. 8).

As can be seen from the figure, the projection of the liquidus surface of this system contains five primary crystallization fields, which are separated from each other by six monovariant curves (Table I). The coordinates of the ten nonvariant equilibria present in the system are provided in the Table II.

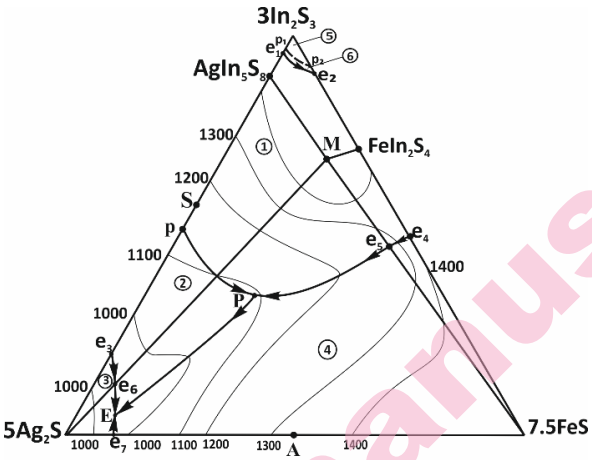

Fig. 8. The liquidus surface of the Ag_2S–In_2S_3–FeS system: 1 – $\varepsilon[\tau(AgIn_5S_8)_{1-x}\beta(In_2S_3)_{x-y}\sigma(FeIn_2S_4)_y]$, 2 – $S(AgInS_2)$, 3 – $\alpha(Ag_2S)$,4 – $\gamma_1(FeS)$, 5 – $\gamma(In_2S_3)$, 6- $\beta(In_2S_3)$

TABLE I. Monovariant reactions in the quasi-ternary system $5Ag_2S$–$3In_2S_3$–7.5FeS

Symbol	Equilibrium	T / K
e_1e_2	$L \leftrightarrow \gamma(In_2S_3) + \sigma(FeIn_2S_4)$	1335-1305
pP	$L \leftrightarrow \sigma(FeIn_2S_4) + S(AgInS_2)$	1130-1050
e_4e_5P	$L \leftrightarrow \sigma(FeIn_2S_4) + \gamma_1(FeS)$	1375-1230-1050
PE	$L \leftrightarrow \gamma_1(FeS) + S(AgInS_2)$	1050-800
e_3e_6E	$L \leftrightarrow S(AgInS_2) + \alpha(Ag_2S)$	945-910-800
e_7E	$L \leftrightarrow \alpha(Ag_2S) + \gamma_1(FeS)$	895-800

TABLE II. Nonvariant reactions in the quasi-ternary system $5Ag_2S$–$3In_2S_3$–7.5FeS

Symbol	Equilibrium	Composition, %			T / K
		$5Ag_2S$	$3In_2S_3$	7.5FeS	
e_1	$L \leftrightarrow \gamma(In_2S_3) + \tau(AgIn_5S_8)$	3.00	97.00	-	1335
e_2	$L \leftrightarrow \gamma(In_2S_3) + \sigma(FeIn_2S_4)$	-	96.00	4.00	1305
e_3	$L \leftrightarrow \alpha(Ag_2S) + S(AgInS_2)$	80.00	20.00	-	945
e_4	$L \leftrightarrow \sigma(FeIn_2S_4) + \gamma_1(FeS)$	-	51.00	49.00	1375
e_5	$L \leftrightarrow \tau(AgIn_5S_8) + \gamma_1(FeS)$	6.00	46.50	47.50	1230
e_6	$L \leftrightarrow \alpha(Ag_2S) + S(AgInS_2)$	83.00	13.00	4.00	910
e_7	$L \leftrightarrow \alpha(Ag_2S) + \gamma_1(FeS)$	91.50	-	8.50	895
E	$L \leftrightarrow \alpha(Ag_2S) + \gamma_1(FeS) + S(AgInS_2)$	88.00	5.00	7.00	800
p	$L + \tau(AgIn_5S_8) \leftrightarrow S(AgInS_2)$	43.00	57.00	-	1130
P	$L + \tau(AgIn_5S_8) \leftrightarrow S(AgInS_2) + \gamma_1(FeS)$	36.50	39.00	24.50	1050

The monovariant equilibrium curves were constructed based on the intersection points of the primary crystallization curves in the sections, and their

direction was extrapolated according to the projections of the monovariant equilibrium curves drawn to the nonvariant equilibrium points and the sides of the concentration triangle. In the projection of the liquidus surface, isotherms were drawn every 100 K by graphical interpolation. The direction of the monovariant equilibrium curves characterizing co-crystallization and the nature of the nonvariant equilibrium points are consistent with the geometric parameters of the liquidus surface projection of the Ag_2S–In_2S_3–FeS ternary system.

CONCLUSION

The quasi-ternary Ag_2S–In_2S_3–FeS system was investigated along polythermal sections. The phase diagrams of the sections and the projection of the liquidus surface were constructed. It was found that the system contains six primary crystallization fields, which are bounded by seven monovariant curves. Among the ten nonvariant equilibria present in the system, seven are three-phase binary eutectics, one is a three-phase binary peritectic, one is a four-phase ternary peritectic, and one is a four-phase ternary eutectic equilibrium. The τ solid solution, crystallizing in the cubic system with a spinel-type structure, occupies a large area in the projection. This solid solution and resulting ternary compounds, may hold potential for applications in the electronics industry due to their photoelectric and magnetic properties.

И З В О Д

ПРОЈЕКЦИЈА ЛИКВИДУСНЕ ПОВРШИНЕ КВАЗИТЕРНАРНОГ Ag_2S–In_2S_3–FeS СИСТЕМА

IKHTIYAR B. BAKHTIYARLY*, SHAHRI S. ABDULLAYEVA, RUKSANA C. QURBANOVA, VILAYET S. MAMMADOV И ELNARA N. ISMAYILOVA

Institute of Catalysis and Inorganic Chemistry named after Academician M. Naghiyev of the Ministry of Science and Education of the Republic of Azerbaijan, Baku, Azerbaijan.

За испитивање квазитернарног система Ag_2S–In_2S_3–FeS дуж политермалног пресека, по први пут су примењене комплексне методе физичко-хемијске анализе, укључујући диференцијалну термичку анализу (DTA), рендгенску дифракциону анализу (XRD), микроструктурну анализу (MSA), као и мерења микротврдоће и густине. Утврђена је природа хемијских интеракција у систему, а конструисани су фазни дијаграм политермалног пресека, као и пројекција ликвидусне површине квазитернарног система. У испитиваном систему одређене су координате инваријантних тачака, моноваријантне криве, границе поља примарне кристализације и изотерме. Утврђено је да се систем састоји од шест поља примарне кристализације, која су ограничена са седам моноваријантних кривих. Од десет утврђених инваријантних равнотежа у систему, седам одговара трофазним бинарним еутектичким, једна трофазној бинарној перитектичкој, једна четворофазној тернарној перитектичкој и једна четворофазној тернарној еутектичкој реакцији.

(Примљено 4. маја; ревидирано 4. јуна; прихваћено 13. августа 2026.)

REFERENCES

1. N. V. Melnikova, L. A. Saipulaeva, P. P. Khokhlachev, A. Yu. Mollaev, A. G. Alibekov, K. V. Kurochka, O. L. Kheifets, A. N. Babushkin *Phys. Solid State* **57** (2015) 2025 (https://doi.org/10.1134/S1063783415100200)
2. S. V. Trukhanov, I. V. Bodnar, M. A.Zhafar, *J. Magn. Magn. Mater.* **379** (2015) 22 (https://doi.org/10.1016/j.jmmm.2014.10.120)
3. L. Wang, Z. Guan, A. Tang, *J. Nanoparticle Res.* **22** (2020) 28 (https://doi.org/10.1007/s11051-019-4724-x)
4. Y. Zhang, H. Zhang, *J. Mater. Chem. C* **9** (2021) 15 (https://doi.org/10.1039/C0TC03435J)
5. M. Kong, A. Osvet, A. Barabash, K. Zhang, H. Hu, J. Elia, C. Erban, T. Yokosawa, E. Spiecker, M. Batentschuk, C. J. Brabec, *ACS Appl. Mater. Interfaces* **15** (2023) 52746 (https://doi.org/10.1021/acsami.3c11140)
6. Y. Hamanaka, T. Ogawa, M. Tsuzuki, T. Kuzuya, *J. Phys. Chem. C* **115** (2011) 1786 (https://doi.org/10.1021/jp110409q)
7. B. Cichy, D. Wawrzynczyk, M. Samoc, W. Stręk, *J. Mater. Chem. C* **5** (2017) 149 (https://doi.org/10.1039/C6TC03854A)
8. Q. Zhang, M. Wang, A. Meiying, Y. Luo, A. Zhang, L. Zhao, L. Yan, F. Deng, X. Luo, *J. Alloys Compd.* **805** (2019) 41 (https://doi.org/10.1016/j.jallcom.2019.06.331)
9. M. Jiao, Y. Li, Y. Jia, C. Li, H. Bian, L. Gao, P. Cai, X. Luo, *J. Colloid Interface Sci.* **565** (2020) 35 (https://doi.org/10.1016/j.jcis.2020.01.006)
10. V. Dzhagan, O. Selyshchev, O. Raievskan, O. Stroyuk, L. Hertling, N. Mazur, M. Y. Valakh, D. R. T. Zahn, *J. Phys. Chem. C* **124** (2020) 15511 (https://doi.org/10.1021/acs.jpcc.0c03268)
11. C. Zhang, Y. Dou, J. Chen, S. Fang, W. Xu, X. Wu, L. Hu, F. Liu, Y. Li, J. Li, *Mater. Today Energy* **27** (2022) 101029 (https://doi.org/10.1016/j.mtener.2022.101029)
12. A. F. Qasrawi, *Thin Solid Films* **519** (2011) 3768 (https://doi.org/10.1016/j.tsf.2010.12.153)
13. X. Sun, M. Shi, C. Zhang, J. Yuan, M. Yin, S. Du, S. Yu, B. Ouyang, F. Xue, S. T. Yang, *ACS Appl. Nano Mater*. **4** (2021) 1029 (https://doi.org/10.1021/acsanm.0c02542)
14. Y. Duan, J. Sun, *Biomimetics* **177** (2023) 1 (https://doi.org/10.3390/biomimetics8020177)
15. V. P. Sachanyuk, G. P. Gorgut, V. V. Atuchin, I. D. Olekseyuk, O. V. Parasyuk, *J. Alloys Compd.* **452** (2008) 348 (https://doi.org/10.1016/j.jallcom.2006.11.043)
16. G. Chen, J. Cheng, C. Jiang, Q. Ye, X. Meng, H. Tang, F. Zhai, L. Li, *J. Mater. Chem. C* **13** (2025) 6980 (https://doi.org/10.1039/D4TC04930F)
17. S. Wang, H. Li, X. Sun, Y. Xu, *Solid State Commun.* **284** (2018) 20 (https://doi.org/10.1016/j.ssc.2018.09.005)
18. G. Delgado, A. J. Mora, C Pineda, T. Tinoco, *Mater. Res. Bull*. **36** (2001) 2507 (https://doi.org/10.1016/S0025-5408(01)00741-3)
19. P. Q. Rustamov, P. K. Babaeva, M. R. Allazov, *Russ. J. Inorg. Chem.* **24** (1979) 2208 (In Russ.)
20. L. A. Taylor, *The System Silver-Iron-Sulfur: Phase Equilibria and Geologic Applications*, Ph.D. Dissertation, Lehigh University, Bethlehem, 1968
21. S. I. Sadovnikov, A. I. Gusev, A. A. Rempel, *Superlatt. Microstruct.* **3** (2015) 35 (https://doi.org/10.1016/j.spmi.2015.03.024)

22. G. A. Steigmann, H. H. Sutherland, J. Goodyear, *Acta Crystallogr*. **19** (1965) 967 (https://doi.org/10.1107/S0365110X65004735)
23. S. J. Kuhn, M. K. Kidder, D. S. Parker, C. dela Cruz, M. A. McGuire, W. M. Chance, L. Li, L. Debeer-Schmitt, J. Ermentrout, K. C. Littrell, M. R. Eskildsen, A. S. Sefat, *Physica C: Supercond. Appl.* **534** (2017) 29 (https://doi.org/10.1016/j.physc.2016.12.006)
24. I. B. Bakhtiyarly, R. J. Kurbanova, Sh. S. Abdullaeva, Z. M. Mukhtarova, F. M. Mammadova, *Condens. Matter Interphases* **23** (2021) 16 (https://doi.org/10.17308/kcmf.2021.23/3293)
25. Sh. S. Abdullayeva, F. M. Mammadov, I. B. Bakhtiyarly, *Russ. J. Inorg. Chem.* **65** (2020) 100 (https://doi.org/10.1134/s0036023619110020)
26. Sh. S. Abdullaeva, I. B. Bakhtiyarly, R. J. Kurbanova, Z. M. Mukhtarova, *Condens.Matter Interphases* **24** (2022) 182 (https://doi.org/10.17308/kcmf.2022.24/000)
27. E. N. Ismailova, L. F. Mashadiyeva, I. B. Bakhtiyarly, M. B. Babanly, *Condens. Matter Interphases* **25** (2023) 47 (https://doi.org/10.17308/kcmf.2023.25/10973)
28. E. N. Ismayilova, L. F. Mashadiyeva, I. B. Bakhtiyarly, V. A. Gasymov, *Condens. Matter Interphases* **27** (2025) 606 (https://doi.org/10.17308/kcmf.2025.27/13298)
29. Ch. I. Abilov, I. B. Bakhtiyarly, S. H. Sadigova, M. Sh. Hasanova, E. K. Gasimova, *J. Serb. Chem. Soc*. **90** (2025) 1119 (https://doi.org/10.2298/JSC250305045A)
30. I. D. Olekseyuk, O. V. Parasyuk, V. R. Kozer, *Khim. nauky* **24** (2009) 3 (In Ukrainian)
31. T. H. Barugu, *Doklady BGUIR* **4** (2018) 18 (In Russian) (https://doklady.bsuir.by/jour/article/view/991/991)
32. V. Ya. Anosov, M. I. Ozerova, Yu. Ya. Fialkov, *Osnovy fiziko-khimicheskogo analiza*, Nauka, Moscow, Russia, 1976, p. 503
33. H. G. Ansell, R. S. Boorman, *J. Electrochem. Soc.* **118** (1971) 133 (https://doi.org/10.1149/1.2407925)
34. P. Pistor, J. M. Merino Alvarez, M. Leon, M. di Michiel, S. Schorr, R. Klenka and S. Lehmann, *Acta Crystallogr. B: Struct. Sci. Cryst. Eng. Mater.* **72** (2016) 410 (https://doi.org/10.1107/S2052520616007058)
35. T. Asikainen, M. Ritala, M. Leskelä, *Appl. Surf. Sci.* **245** (2005) 122 (https://doi.org/10.1016/0169-4332(94)90206-2)
36. M. G. Sandoval-Paz, M. Sotelo-Lerma, J. J. Valenzuela-Jáuregui, M. Flores-Acosta, R. Ramírez-Bon, *Thin Solid Films* **472** (2005) 5 (https://doi.org/10.1016/j.tsf.2004.05.096)
37. I. B. Bakhtiyarly, *Chem. Probl.* (2003) 57
38. Kh. S. Mamedov, I. B. Bakhtiyarov, Crystal Chemical properties peritectic compounds *Twelfth (XII) Europen crystallographic mecting. Collected abstracts Moscow, USSR* **2** (1989) 112.